

PREDICTION OF NONLINEAR TIME HISTORY DEFLECTION OF SCALLOP DOMES BY NEURAL NETWORKS

R. Kamyab^{*,†} and E. Salajegheh

*Department of Civil Engineering, Shahid Bahonar University of Kerman, Kerman, Iran
The Iranian Academic Center for Education, Culture and Research, Kerman, Iran*

ABSTRACT

This study deals with predicting nonlinear time history deflection of scallop domes subject to earthquake loading employing neural network technique. Scallop domes have alternate ridged and grooves that radiate from the centre. There are two main types of scallop domes, lattice and continuous, which the latticed type of scallop domes is considered in the present paper. Due to the large number of the structural nodes and elements of scallop domes, nonlinear time history analysis of such structures is time consuming. In this study to reduce the computational burden radial basis function (RBF) neural network is utilized. The type of inputs of neural network models seriously affects the computational performance and accuracy of the network. Two types of input vectors: cross-sectional properties and natural periods of the structures can be employed for neural network training. In this paper the most influential natural periods of the structure are determined by adaptive neuro-fuzzy inference system (ANFIS) and then are used as the input vector of the RBF network. Results of illustrative example demonstrate high performance and computational accuracy of RBF network.

Received: 6 July 2011; Accepted: 4 November 2011

KEY WORDS: earthquake; nonlinear behaviour; radial basis function; adaptive neuro-fuzzy inference system; neural network

1. INTRODUCTION

Dynamic analysis of structures subject to earthquakes is usually achieved by a step-by-step procedure that determines the history of response of structures which vary with time. Such

*Corresponding author: R. Kamyab Department of Civil Engineering, Shahid Bahonar University, Kerman, Iran and The Iranian Academic Center for Education, Culture and Research, Kerman, Iran

†E-mail address: r_kamyab_m@yahoo.com

processes are called time history methods. Time history analysis of large scale structures requires much computational effort. This drawback will be resonated when the dynamic responses of structures are required to complete an iterative algorithm such as optimisation. Therefore, approximating of the time history responses of structures may effectively reduce the computational burden.

In the recent decade, neural network techniques are widely utilized to simplify the complex problems in a broad range of science and engineering cases. All the neural networks have training and predicting operational modes. In training mode they accept a set of input-target pairs and regulate the adjustable arguments of the networks according to the best mapping relationship between input and target spaces. In predicting mode the trained networks are employed to predict the outputs.

Some neural networks such as radial basis function (RBF), generalized regression (GR), counter propagation (CP), back propagation (BP) and wavelet back propagation (WBP) neural networks are used in civil and structural engineering applications [1-4]. In the field of structural engineering, one of the most popular neural networks is RBF network [5-7]. This network is very interesting due to its rapid training, generality and simplicity [8].

In the last years, RBF neural network are used for predicting linear time history responses of structures subjected to earthquake [9-13]. Also in [14] RBF neural network is employed for predicting nonlinear time history responses of space towers. In this study the most influential natural periods of scallop domes are determined using ANFIS. These important natural periods are employed then as the inputs of the RBF network instead of cross-sectional properties. This task significantly improves the computational performance of the RBF network.

In the numerical example, the inputs and outputs of the RBF neural network are the most influential natural periods of the structures and time history deflection of top node of structures subject to the vertical component of BAM earthquake. In order to provide training data ANSYS [15] are employed, also, to train and test the RBF network and ANFIS, MATLAB [16] is utilized.

2. SCALLOP DOMES

The idea of scallop domes was proposed for the first time by Nooshin *et. al* in [17]. Consider the dome configuration a perspective view of which is shown in Figure 1a. This is a single layer dome whose nodes lie on a spherical cap. The plan view of the dome is shown in Figure 1b [17].

Now, consider the dome configuration shown in Figure 1d. The plan view of this dome is identical to that of the dome of Figure 1a, as given in Figure 1b. Also, the borders of the segments in Figure 1d are identical in shape to the ones in Figure 1a. The difference between the domes of Figures 1a and 1d is that the segments in Figure 1d are arched. More specifically, in the case of the dome of Figure 1d, the nodal points along every circumferential ring are raised vertically such that the part of the ring between the borders in each segment is turned into an arch. The arching effect is such that: The nodal points on the segmental borders remain in their original positions (in particular, the position of the crown of the dome remains

unchanged) and the rise of the arches increases with distance from the crown of the dome. The maximum rise for a circumferential ring, which occurs at the middle of each segment, is referred to as the "amplitude of the ring". The ring that is furthest away from the crown, namely, the "base ring" has the largest amplitude. This amplitude is referred to as the "amplitude of the dome", as indicated in Figure 1d. In this figure, the dotted curve shows the identical position of the base ring before "arching" of the segments. The dome of Figure 1d is an example of a class of domes that are referred to as scallop domes [17].

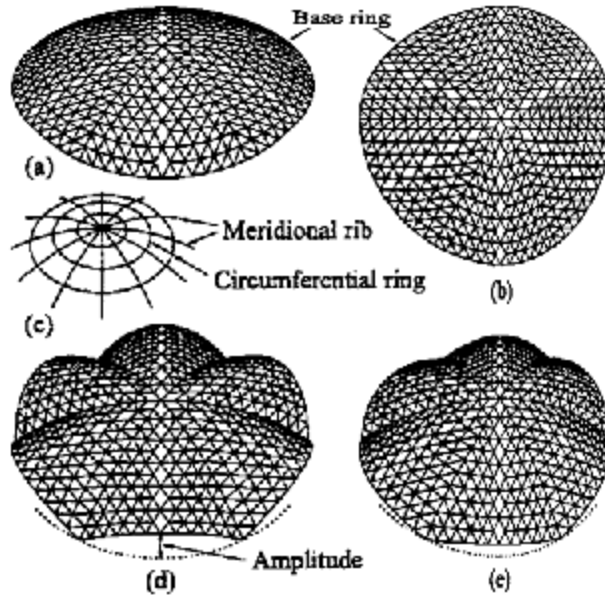


Figure 1. Examples of scallop domes

3. NONLINEAR TIME HISTORY ANALYSIS OF STRUCTURES

Time-history analysis is a step-by-step analysis of the dynamical response of structures to a specified loading that vary with time such as earthquake. Time history analysis against the earthquake determines the dynamic response of structures subject to ground acceleration. The dynamic equilibrium equations that must be solved are given as:

$$M\ddot{U}(t) + C\dot{U}(t) + KU(t) = -MI\ddot{u}_g(t) \tag{1}$$

where M , C and K are the mass, damping and stiffness matrices, respectively; $\ddot{U}(t)$, $\dot{U}(t)$ and $U(t)$ are the acceleration, velocity and displacement vectors of structure; I is unit vector; $\ddot{u}_g(t)$ is the ground acceleration.

The dynamic equilibrium of motion Eq. (1) can be solved by using any of the available numerical integration methods. One of the popular solution methods is the Newmark's integration method.

In order to perform dynamic analysis considering inelastic behavior, ANSYS is employed.

A simple perfectly plastic stress-strain relationship is adopted in order to take into account the transient nature of earthquake loading. Geometric nonlinearity effects are also considered. The perfectly plastic stress-strain relationship is shown in Figure 2.

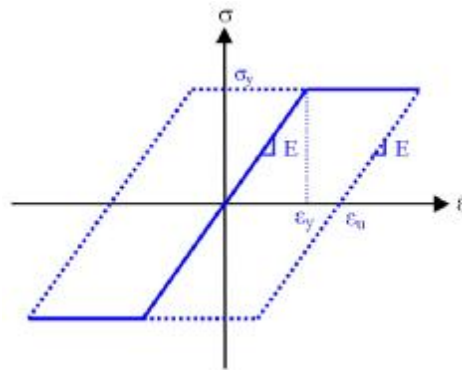


Figure 2. Full plastic stress-strain relationship

Nonlinear time history analysis of large scaled structures, such as scallop domes, is a time consuming process. In this study, in order to reduce the computational burden RBF neural network are employed to predict the desired structural responses.

4. RADIAL BASIS FUNCTION (RBF) NEURAL NETWORK

Radial basis functions (RBFs) take an interesting approach by viewing the design of a neural network as a curve-fitting problem by finding a best fit to the training data in a multidimensional space. RBF networks are two layer feed forward neural networks. The first layer consists of RBF neurons with Gaussian activation functions. The outputs of RBF neurons have significant responses to the inputs only over a range of values of s called the receptive field. The size of the receptive field is determined by the value of σ . The value of σ allows the sensitivity of the RBF neurons to be adjusted. Activation function of RBF neurons is as follows:

$$h_{\xi}(s) = \exp\left(-\frac{(s - c_{\xi})^T (s - c_{\xi})}{2\sigma_{\xi}^2}\right) \quad (2)$$

where s is an input vector, h_{ξ} , c_{ξ} and σ_{ξ} are Gaussian activation function, weight vector and radius of receptive field of ξ th RBF neuron, respectively.

The output layer neurons produce the linear weighted summation of hidden layer neurons responses.

To train the hidden layer of RBF networks no training is accomplished and the transpose of training input matrix is taken as the layer weight matrix [8].

$$C = A^T \quad (3)$$

where, C and Λ are input layer weight matrix and training input matrix, respectively.

The second layer weights are obtained by solving the following matrix equation:

$$\mathbf{T} = \Phi \mathbf{W} \Rightarrow \mathbf{W} = \Phi^{-1} \mathbf{T} \tag{4}$$

where \mathbf{T} , Φ , and \mathbf{W} are the target matrix (desired outputs), the matrix of first layer outputs, and the weight matrix of the second layer.

The numerical results of many scientific and engineering applications indicate that RBF networks are very good tools for interpolation and also their training is very fast.

It is demonstrated in [10-13] that using the natural periods of the structures as the inputs of the RBF network leads to better performance generality. In this study also the natural periods are used as the inputs of the RBF network. As the number of the natural periods of the scallop domes is large, considering all of them as the inputs is impossible. Therefore a computational strategy should be adopted to select the important ones. In this study, ANFIS is employed to achieve this task.

5. ADAPTIVE NEURO-FUZZY INFERENCE SYSTEM (ANFIS)

The ANFIS is a hybrid network which uses neural network learning algorithms and fuzzy reasoning to map inputs into an output. For simplicity, a typical ANFIS architecture with only two inputs leading to four rules and one output for the first order Sugeno fuzzy model is expressed [18-19]. It is also assumed that each input has two associated membership functions (MFs). It is evident that this architecture can be easily generalized to any arbitrary dimensions. The architecture of a typical ANFIS is shown in Figure 3.

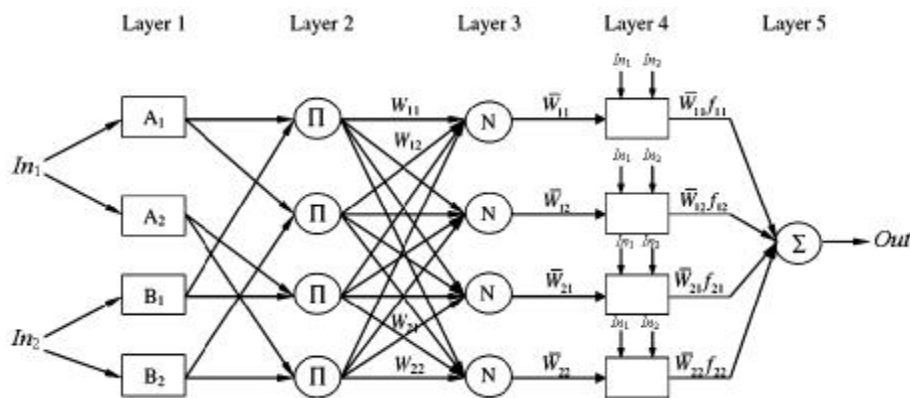


Figure 3. The architecture of a typical ANFIS

Modifiable parameters of the ANFIS architecture are placed in Layers 1 and 4. During the training phase, adjustment of the modifiable parameters is facilitated by a gradient vector. In this study, a hybrid algorithm is employed for training which its mathematical background can

be found in [20].

ANFIS can be used to find the most influential inputs, n_i , from the whole candidates, n_i , affecting an output in the framework of an exhaustive search by building an ANFIS model for each combination of input vector components and training it for a little epoch. In this study, however the aim is to predict the time history nonlinear deflection of the top node, the maximum deflection of each structure, all over the earthquake duration, is considered as the ANFIS output. By using this technique, the dimension of the input vector of the neural networks can be reduced and the accuracy of the prediction is improved. The pseudo code of exhaustive search by ANFIS to determine the most influential inputs is given in [12]. After finding the most influential inputs, they can be employed as the inputs instead of the initial inputs, in the training phase of neural network models. In this case, as the number of input vector components is reduced, the training process is efficiently achieved.

6. EVALUATION METRICS

In order to evaluate the accuracy of the approximate structural responses obtained by RBF neural networks, two evaluation metrics are used:

The RRMSE error between the exact and approximate responses is defined as follows:

$$RRMSE = \left(\frac{\frac{1}{r-1} \sum_{\eta=1}^r (u_{\eta} - \tilde{u}_{\eta})^2}{\frac{1}{r} \sum_{\eta=1}^r (u_{\eta})^2} \right)^{\frac{1}{2}} \quad (5)$$

$$R^2 = 1 - \left(\frac{\sum_{\eta=1}^r (u_{\eta} - \tilde{u}_{\eta})^2}{\sum_{\eta=1}^r (u_{\eta} - \bar{u})^2} \right) \quad (6)$$

where u_{η} and \tilde{u}_{η} are the η th component of the exact and approximate responses, respectively. The mean value of exact vectors component and the vectors dimension are expressed by \bar{u} and r , respectively.

7. NUMERICAL RESULTS

In this study a scallop dome with the span of 44.32m and the height of 7.63 m, shown in Figure 4, is considered. Young's modulus and mass density are 2.1×10^{10} kg/m² and 7850 kg/m³, respectively. The computational time is measured in terms of CPU time required by a PC Pentium IV 3000 MHz.

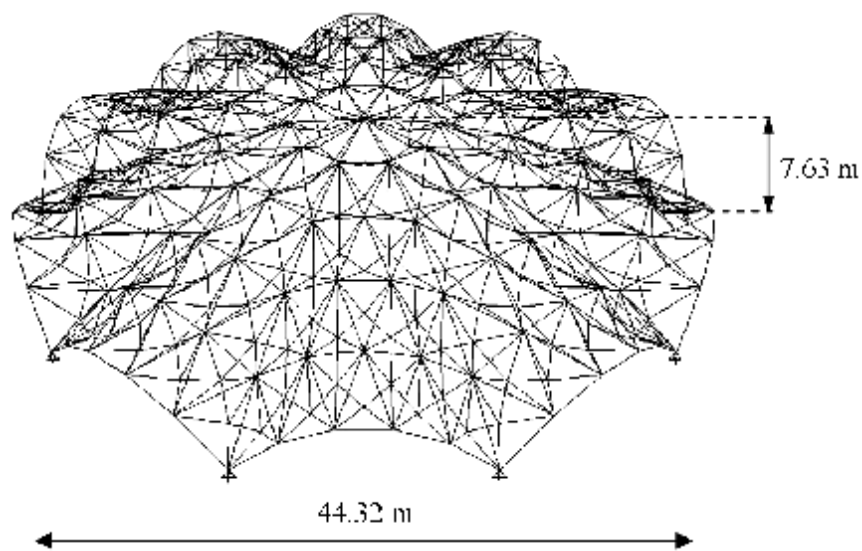


Figure 4. The considered scallop dome

All the structural members of top, web and bottom layers are grouped in groups 1, 2 and 3, respectively. These groups are shown in Figure 5.

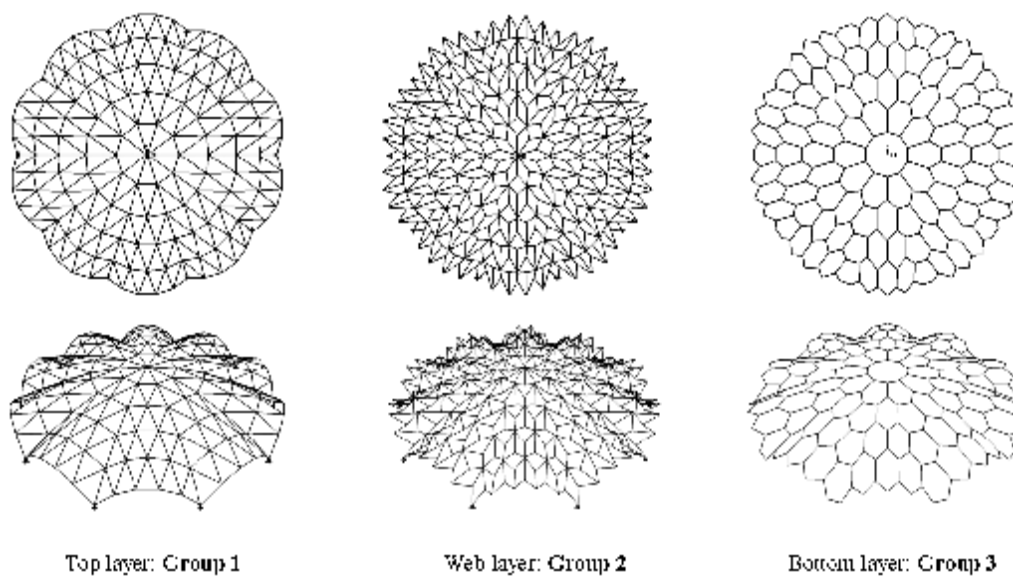


Figure 5. The structural elements' groups

The available standard pipe profiles for this example are listed in Table 1. In this study, vertical component of Bam earthquake (Iran-2003) is considered. This component of the earthquake contains 13310 points with the PGA of 9.885 m/s^2 . Here a portion of the earthquake with 1500 points shown in Figure 6 is considered.

Table 1: Available standard pipe profiles

No.	d (mm)	t (mm)	A (cm ²)	No.	d (mm)	t (mm)	A (cm ²)
1	33.7	2.6	2.54	9	101.6	4.0	12.30
2	42.4	2.6	3.25	10	88.9	5.0	13.20
3	48.3	3.2	4.53	11	88.9	6.0	15.60
4	48.3	4.0	5.57	12	88.9	6.3	16.30
5	60.3	4.0	7.07	13	114.3	5.0	17.20
6	60.3	5.0	8.69	14	101.6	6.3	18.90
7	76.1	4.0	9.06	15	114.3	6.3	21.40
8	88.9	4.0	10.70	16	114.3	8.0	26.70

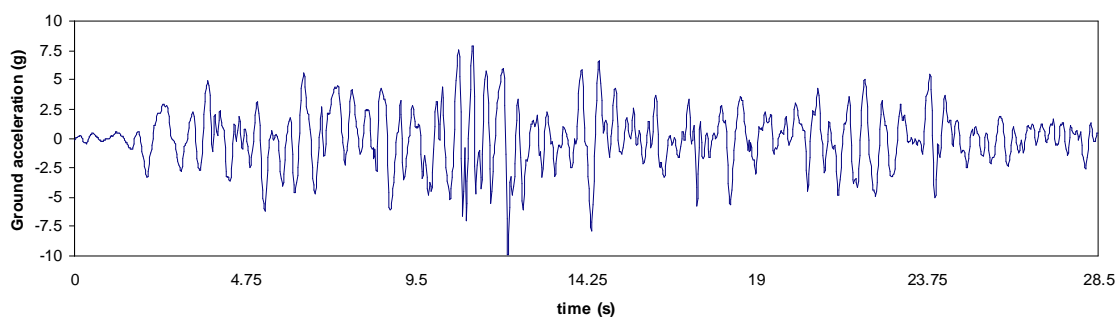


Figure 6. Vertical component of Bam earthquake (Iran-2003)

In order to train RBF neural network to predict the nonlinear time history displacement of the top node of the structure, 100 samples are randomly generated based on groups 1 to 3 cross-sectional-areas. The selected structures are analyzed for the Bam earthquake record using nonlinear FE method and Newmark scheme. The spent time in this stage is 800.0 min. Cross-sectional-areas of the selected 100 structures are given in Table 2. In this table, the structures which loss their overall stability during the nonlinear time history analysis are shown by F and otherwise by S. It can be observed from 100 structures, in analysing 12 ones, the convergence is not met and these structures loss their stability subject to earthquake. From 88 safe structures, 79 and 9 ones are randomly selected for training and testing, respectively.

In order to achieve an exhaustive search to find important natural periods, the first 50 natural periods are selected, $n_i = 50$.

$$In_{ANFIS} = \{T_1 \ T_2 \ \dots \ T_{50}\}^T \quad (7)$$

$$Out_{ANFIS} = \max\{d(t_i), i=1,2,\dots,nep\} \quad (8)$$

where, T , d and nep are natural period, deflection and the number of earthquake points, respectively.

Table 2: Selected structures

No.	A ₁	A ₂	A ₃	Failed/Safe	No.	A ₁	A ₂	A ₃	Failed/Safe
1	18.9	21.4	4.53	S	51	9.06	2.54	21.4	S
2	21.4	15.6	3.25	S	52	26.7	10.7	10.7	S
3	7.07	12.3	26.7	S	53	8.69	21.4	8.69	S
4	26.7	4.53	26.7	S	54	3.25	17.2	9.06	F
5	26.7	10.7	17.2	S	55	5.57	9.06	3.25	F
6	4.53	9.06	21.4	S	56	4.53	26.7	26.7	S
7	17.2	26.7	15.6	S	57	13.2	2.54	5.57	S
8	2.54	18.9	21.4	S	58	8.69	18.9	2.54	S
9	15.6	17.2	16.3	S	59	2.54	4.53	15.6	F
10	9.06	15.6	4.53	S	60	16.3	15.6	10.7	S
11	16.3	2.54	7.07	S	61	12.3	7.07	16.3	S
12	2.54	3.25	18.9	F	62	5.57	15.6	4.53	S
13	16.3	8.69	26.7	S	63	8.69	15.6	17.2	S
14	2.54	10.7	9.06	S	64	3.25	21.4	17.2	S
15	17.2	17.2	4.53	S	65	10.7	9.06	10.7	S
16	10.7	10.7	15.6	S	66	7.07	12.3	12.3	S
17	16.3	17.2	7.07	S	67	18.9	17.2	15.6	S
18	15.6	15.6	4.53	S	68	9.06	17.2	12.3	S
19	3.25	10.7	26.7	S	69	8.69	26.7	21.4	S
20	8.69	13.2	5.57	S	70	12.3	13.2	13.2	S
21	17.2	7.07	12.3	S	71	5.57	7.07	10.7	S
22	16.3	21.4	26.7	S	72	5.57	18.9	5.57	S
23	12.3	4.53	4.53	S	73	5.57	4.53	5.57	S
24	7.07	18.9	7.07	S	74	9.06	7.07	21.4	S
25	18.9	5.57	21.4	S	75	9.06	4.53	21.4	S
26	8.69	5.57	7.07	S	76	26.7	10.7	3.25	S
27	13.2	10.7	8.69	S	77	7.07	9.06	13.2	S
28	18.9	13.2	12.3	S	78	7.07	13.2	16.3	S
29	21.4	7.07	17.2	S	79	5.57	3.25	7.07	F
30	17.2	9.06	13.2	S	80	8.69	9.06	12.3	S
31	3.25	2.54	12.3	F	81	3.25	7.07	17.2	F
32	17.2	21.4	4.53	S	82	2.54	21.4	16.3	S
33	13.2	10.7	2.54	S	83	10.7	13.2	5.57	S
34	8.69	4.53	17.2	S	84	10.7	26.7	12.3	S
35	7.07	12.3	4.53	S	85	12.3	5.57	10.7	S
36	13.2	7.07	15.6	S	86	13.2	15.6	9.06	S
37	16.3	16.3	10.7	S	87	8.69	26.7	2.54	S
38	3.25	5.57	21.4	S	88	21.4	21.4	17.2	S
39	4.53	18.9	12.3	S	89	3.25	7.07	8.69	S
40	26.7	3.25	10.7	S	90	15.6	4.53	16.3	S
41	3.25	26.7	2.54	F	91	3.25	15.6	10.7	S
42	17.2	18.9	18.9	S	92	17.2	16.3	21.4	S
43	3.25	9.06	7.07	S	93	21.4	8.69	16.3	S
44	17.2	9.06	21.4	S	94	5.57	2.54	16.3	F
45	4.53	7.07	4.53	F	95	12.3	10.7	21.4	S
46	4.53	18.9	13.2	S	96	13.2	13.2	18.9	S
47	12.3	4.53	18.9	S	97	17.2	13.2	4.53	S
48	13.2	8.69	12.3	S	98	5.57	21.4	2.54	S
49	9.06	3.25	5.57	F	99	10.7	4.53	26.7	S
50	3.25	4.53	5.57	F	100	16.3	12.3	10.7	S

In this case, four influential natural periods are determined as follows:

$$In_{inf} = \{T_3 \ T_5 \ T_{17} \ T_{29}\}^T \quad (9)$$

The spent time in this stage is about 72.0 min.

Two RBF neural network models, RBF and RBF+ANFIS, are trained for predicting the nonlinear time history deflection of the top node of the scallop dome. The actual and predicted responses of the mentioned test samples by RBF+ANFIS are compared in Figures 7 to 15.

Table 3: Testing results

No.	Sample No. in Table 2.	RBF		RBF+ANFIS	
		Rrmse	R ²	Rrmse	R ²
1	61	0.9984	0.0392	0.9976	0.0491
2	15	0.9604	0.1988	0.9980	0.0438
3	58	0.9855	0.1202	0.9983	0.0408
4	68	0.9089	0.3017	0.9859	0.1188
5	35	0.9994	0.0003	0.9998	0.0001
6	21	0.9287	0.2670	0.9899	0.1002
7	84	0.9751	0.1576	0.9961	0.0621
8	12	0.9930	0.0834	0.9975	0.0494
9	46	0.9297	0.2857	0.9899	0.1003
mean	-	0.9643	0.1615	0.9948	0.0627

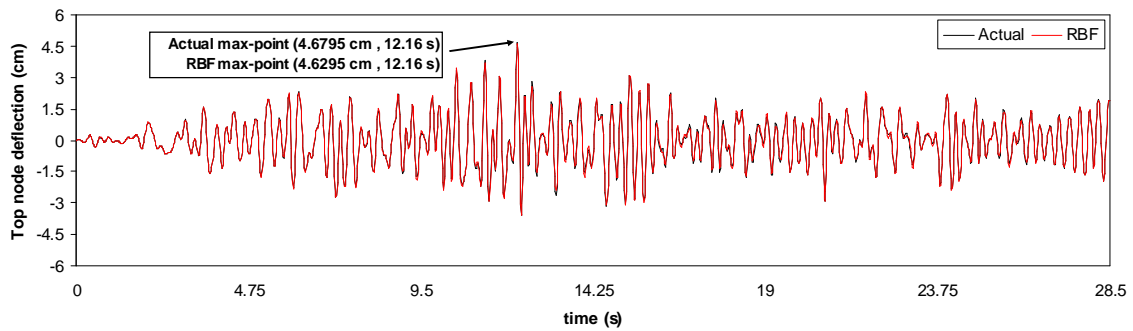


Figure 7. Actual top node deflection vs. predicted one by RBF neural network for 1st test sample

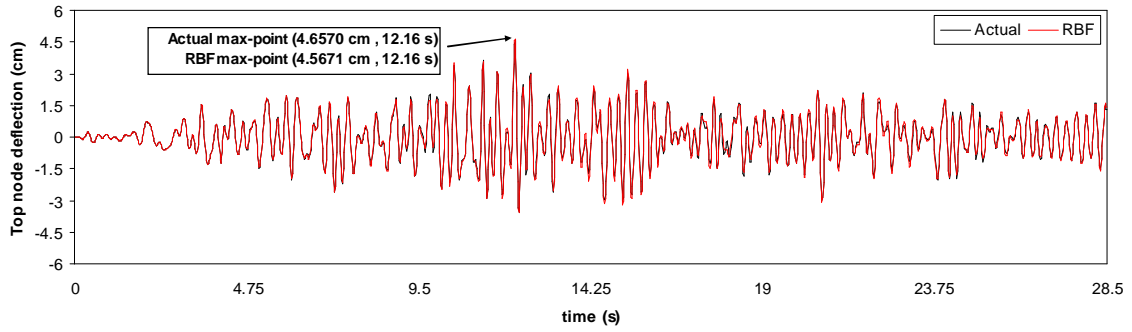


Figure 8. Actual top node deflection vs. predicted one by RBF neural network for 2nd test sample

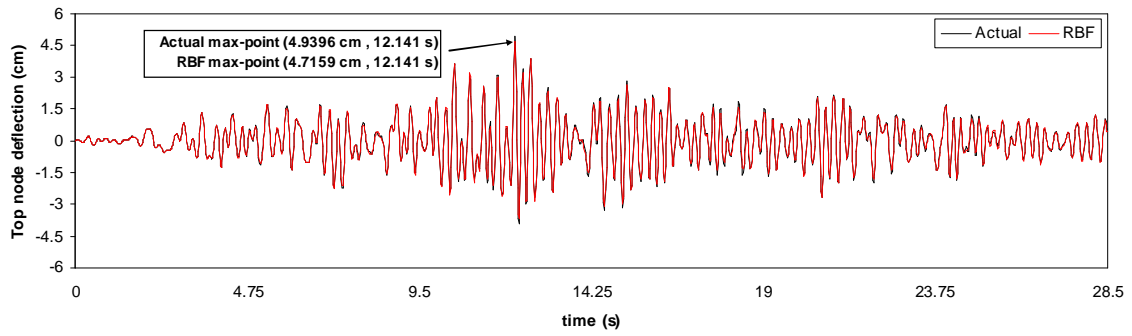


Figure 9. Actual top node deflection vs. predicted one by RBF neural network for 3rd test sample

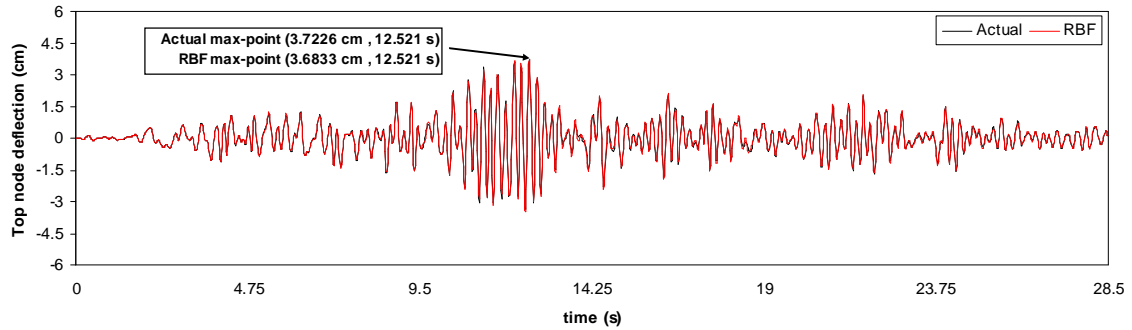


Figure 10. Actual top node deflection vs. predicted one by RBF neural network for 4th test sample

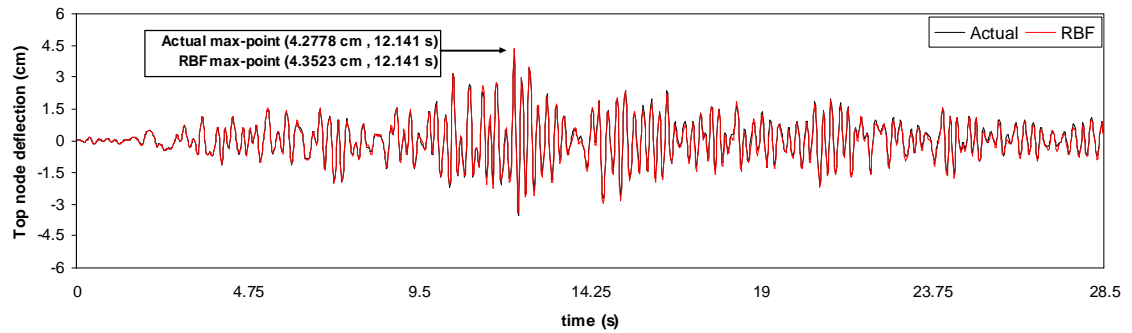


Figure 11. Actual top node deflection vs. predicted one by RBF neural network for 5th test sample

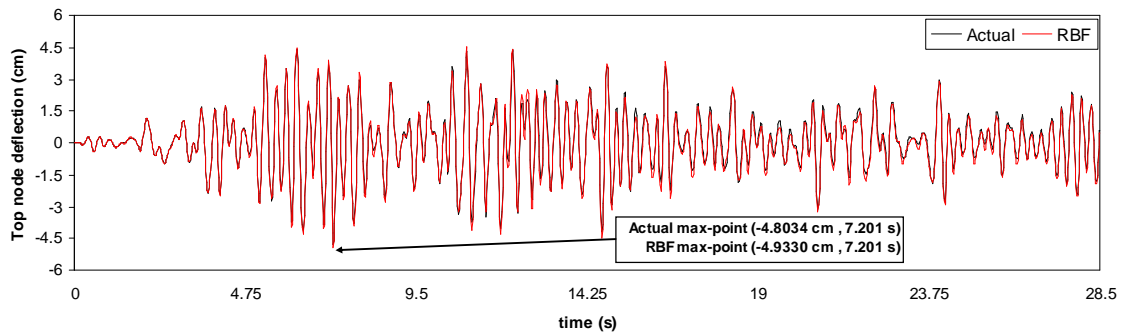


Figure 12. Actual top node deflection vs. predicted one by RBF neural network for 6th test sample

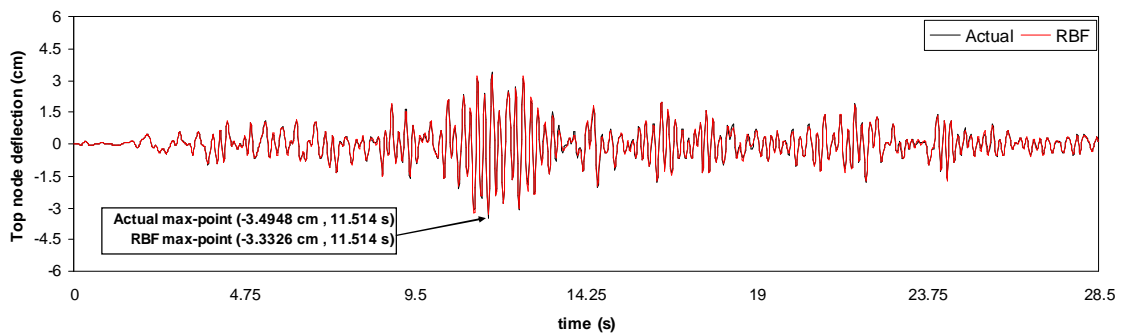


Figure 13. Actual top node deflection vs. predicted one by RBF neural network for 7th test sample

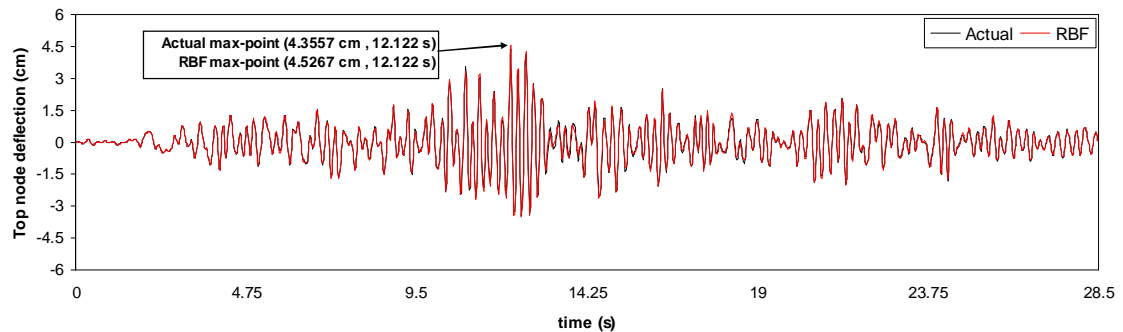


Figure 14. Actual top node deflection vs. predicted one by RBF neural network for 8th test sample

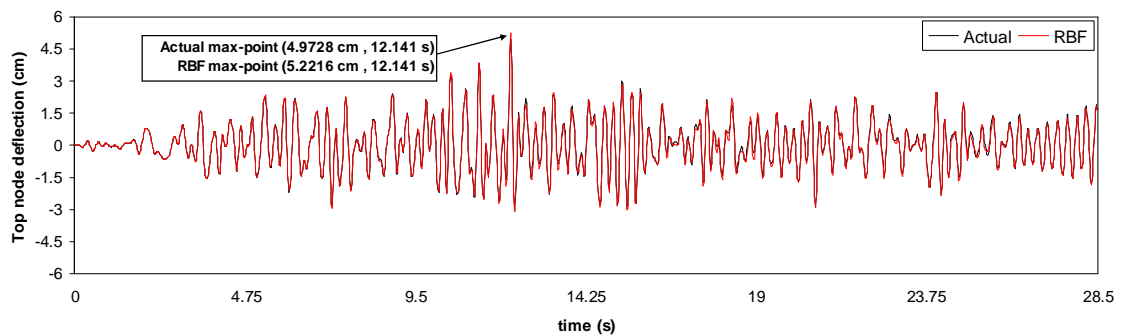


Figure 15. Actual top node deflection vs. predicted one by RBF neural network for 9th test sample

8. CONCLUSION

An efficient methodology is introduced for predicting nonlinear time history deflection of scallop domes subject to earthquake loads by the main goal of reducing the computational burden. As the scallop domes are large scaled structures, nonlinear time history analysis of these structures is time consuming. Radial basis function (RBF) neural network is employed to reduce the computational effort. Also, the most influential natural periods of the structure are determined by adaptive neuro-fuzzy inference system (ANFIS) and then are used as the input vector of the RBF network. In this case two neural network models: RBF and RBF+ANFIS are used to predict the responses. Numerical results indicate that the generalization of the RBF+ANFIS model is better than that of the RBF model.

REFERENCES

1. Salajegheh E, Gholizadeh S. Optimum design of structures by an improved genetic algorithm and neural networks. *Adv Eng Softw*, 2005; **36**(11-12):757-67.
2. Salajegheh E, Heidari A. Optimum design of structures against earthquake by wavelet neural network and filter banks. *Earthquake Eng Struct*, 2005; **34**(1):67-82.
3. Fang X, Luo H, Tang J. Structural damage detection using neural network with learning rate improvement. *Comput Struct*, 2005; **83**(25-26):2150-61.
4. Lanzi L, Bisagni C, Ricci S. Neural network systems to reproduce crash behavior of structural components. *Comput Struct*, 2004; **82**(1):93-108.
5. Deng J. Structural reliability analysis for implicit performance function using radial basis function network. *Int J Solids Struct*, 2006; **43**(11-12):3255-91.
6. Roy N, Ganguli R. Filter design using radial basis function neural network and genetic algorithm for improved operational health monitoring. *Appl Soft Comput*, 2006; **6**(2):154-69.
7. Zhang A, Zhang L. RBF neural networks for the prediction of building interference effects. *Comput Struct*, 2004; **82**(27):2333-9.
8. Wasserman PD. *Advanced Methods in Neural Computing*. New York: Prentice Hall Company, Van Nostrand Reinhold, 1993.
9. S. Gholizadeh, O.A. Samavati. Structural optimization by wavelet transforms and neural networks. *Appl Math Model*, 2011; **35**:915-29.
10. Gholizadeh S, Salajegheh E. Optimal design of structures for earthquake loading by self organizing radial basis function neural networks. *Adv Struct Eng*, 2010; **13**:339-56.
11. S. Gholizadeh, E. Salajegheh. Optimal seismic design of steel structures by an efficient soft computing based algorithm. *J Constr Steel Res*, 2010; **66**:85-95.
12. S. Gholizadeh, E. Salajegheh. Optimal design of structures for time history loading by swarm intelligence and an advanced metamodel. *Comput Meth Appl Mech*, 2009; **198**:2936-49.
13. Gholizadeh S, Salajegheh J, Salajegheh E. An intelligent neural system for predicting structural response subject to earthquakes. *Adv Eng Softw*, 2009; **40**:630-9.
14. S. Gholizadeh. Structural optimization for earthquake loading with nonlinear responses

- by surrogate modeling based evolutionary algorithms. *Asian J Civil Eng*, 2010; **11**:25-42.
15. ANSYS Incorporated. ANSYS Release 8.1. 2004.
 16. The Language of Technical Computing. MATLAB. Math Works Inc, 2006.
 17. Nooshin H, Tomatsuri H, Fujimoto, M. Scallop domes. IASS97 Symposium on Shell & Spatial Structures: Design, Performance & Economics, Singapore, 1997.
 18. Wang YM, Elhag T. An adaptive neuro-fuzzy inference system for bridge risk assessment. *Expert Syst Appl*, 2008; **34**:3099-106.
 19. Sugeno M. *Industrial Applications of Fuzzy Control*. Elsevier Science Pub. Co, 1985.
 20. Jang JSR. ANFIS: Adaptive-network-based fuzzy inference systems. *IEEE Transactions on Systems Man and Cybernetics* 1993; **23**:665–85.